Manuscript prepared for Atmos. Chem. Phys. Discuss.
with version 2014/09/16 7.15 Copernicus papers of the LaTeX class copernicus.cls.
Date: 7 April 2015

A case study of a low level jet during OPALE

H. Gallée, H. Barral, E. Vignon, and C. Genthon

CNRS/UJF – Grenoble 1, Laboratoire de Glaciologie et Géophysique de l'Environnement (LGGE), France

Correspondence to: H. Gallée (gallee@lgge.obs.ujf-grenoble.fr) and C. Genthon (genthon@lgge.obs.ujf-grenoble.fr)

Abstract

A case study of a low level jet during the OPALE (Oxidant Production over Antarctic Land and its Export) summer campaign is presented. It has been observed at Dome C (East Antarctica) and is simulated accurately by the three-dimensional version of the Modèle Atmosphérique Régional (MAR). It is found that this low level jet is not related to an episode of thermal wind, conforting that Dome C may be a place where turbulence on flat terrain can be studied.

1 Introduction

Low Level Jets (LLJs) have been observed and studied for a long time (see e.g., Davies, 2000; Cuxart and Jimenez, 2006; Banta et al., 2003). Their interest may be related to the need of a better understanding of the atmospheric boundary layer. On one hand they are suspected to generate additional turbulence. On the other hand their behaviour may have an impact among others on the management of wind turbines, birds migration (Van de Wiel et al., 2010). Following Blackadar (1957) and Van de Wiel et al. (2010) LLJs may be due to the onset of an inertial oscillation when the turbulence force suddenly decreases at the end of day-time. LLJs have been observed over the Weddel Sea (Antarctica) (Andreas et al., 2000).

A wind speed maximum near the surface has also been observed at South Pole during ANTCI (Neff et al., 2008). In constrast with the LLJs observed at Dome C it is associated to events of inversion winds. Indeed South Pole is situated on a slope, while Dome C is not. The LLJ at Dome C is related to the pressure gradient force (PGF) extending well above the boundary layer while at South Pole the wind speed maximum is caused by the downslope PGF developing only in the bulk of the inversion winds layer. Another difference is that there is no diurnal cycle at South Pole. Consequently a LLJ could not develop there at the end of day-time, when turbulence shuts down. Possibly a LLJ could develop at South Pole with a rapid stabilization of the atmosphere associated with changes in synoptic scale conditions.

A consequence of the absence of a diurnal cycle is that turbulence in the stable boundary layer of South Pole may reach an equilibrium, while this is not the case at Dome C during summer. Note that Neff et al. (2008) mention that the behavior of nitrous oxyde (NO) below the wind speed maximum they observe is not fully understood since it could depend (but not always) on an accumulation process of NO over a thin drainage flow which thickness increases gradually before it reaches South Pole. In our case no drainage flow reaches Dome C so that the above-mentioned accumulation process does not exist.

A common point between LLJs associated with an inertial oscillation and the observations of Neff et al. (2008) is that the wind shear is zero at the jet maximum, so that turbulent transport could not exist through the jet core (gradient Richardson number is "infinite" there). Note however that the LLJ at Dome C forms at a height where turbulence has already shut down, so that the LLJ is not strictly necessary for precluding vertical turbulent transport there. In contrast the wind speed maximum at South Pole is associated to the turbulent inversion winds, and could play a more important role in causing the shutdown of turbulence.

Finally the shutdown of turbulence by a wind speed maximum remains an open question. Indeed turbulence bursts have been simulated through a jet core in a LES by Cuxart and Jiménez (2007), but only when the wind and air temperature near the surface are prescribed in their model.

In this note we consider a case study of a low level jet happening at Dome C during the night of 16–17 December 2011 (during OPALE campaign) and accurately simulated by MAR. The model has been satisfactorily validated for the OPALE campaign in Gallée et al. (2014, this issue). The objective here is to focus on the driving forces of a LLJ at Dome C.

2 The model

The model used is MAR (Modèle Atmosphérique Régional). It is described and set up as in Gallée et al. (2014, this issue). A summary is given here.

MAR is a hydrostatic primitive equations model using finite differences schemes (Gallée and Schayes, 1994). The terrain following normalized pressure is used to take into account topography. Turbulence is parametrized by using two prognostic equations for turbulent kinetic energy and its dissipation (Duynkerke, 1988; Bintanja, 2000). The prognostic equation of dissipation allows to relate the mixing length to local sources of turbulence and not only to the surface. Finally the relationship between the turbulent diffusion coefficient for momentum and scalars (Prandtl number) is dependant on the Richardson number, according to Sukoriansky et al. (2005). An explicit cloud microphysical scheme describes exchanges between water vapor, cloud droplets, cloud ice crystals (concentration and number), snow particles and rain drops (Gallée, 1995).

The horizontal domain covers an area of about $800\,\mathrm{km} \times 800\,\mathrm{km}$ surrounding Dome C. The x axis of MAR domain is directed from the south-west to the north-east (see Fig. 1 – see also Fig. 3 for a localisation of Dome C over the Antarctic ice sheet). Horizontal grid size is 20 km. There are 60 levels, with a vertical discretization in the lower troposphere of 2 m. It decreases with altitude above 32 m a.g.l., reaching 50 m at 300 m a.g.l. and 400 m at 3000 m a.g.l.

The simulation is started on 1 November 2011 and the model is not reinitialized until the end of the experiment (end of January 2012). Thus the simulation is sufficiently long to allow the influence of lateral boundary conditions to reach the central part of the domain, in contrast to what happens in a simulation starting from prescribed initial conditions, and lasting of few hours or days only. As lateral boundary conditions are over-specified in a limited area model, they may distort its solution and cause some differences between the simulation and the observation. This point will be illustrated in the next section.

3 The low level jet

3.1 Overview

It was possible to observe LLJs occurring only at a height below the top of the tower. As LLJs occur where turbulence shuts down this means that in these cases stabilization of the vertical column of air is strong, i.e., when the wind shear is not too large and a strong radiational cooling of the surface occurs.

Observed and simulated LLJs during the OPALE period (12 December 2011 - 14 January 2012) are listed in table 1. They are obtained by searching from below the lowest wind speed maximum below the highest level of the tower. Note that the vertical resolution of the model (2 m) is higher than that of the observations (6 levels, respectively at 3.5 m, 10.8 m, 18.2 m, 25.6 m, 32.9 m and 42.1 m). Consequently the estimation of the height of the LLJ in the observations may be very crude. No LLJ is simulated nor observed in January 2012, but no observations at the tower were made between 1 and 9 January and generally we did not get clear sky conditions in the first half of January 2012 (see e.g. fig. 2a of the companion paper - Gallée et al., 2014). MAR simulated a LLJ on 15 December below the top of the tower while it was very weak in the observation. No LLJ was simulated below the top of the tower on 26, 27 and 28 December, when MAR underestimated cloud cover and consequently overestimated day-time solar warming the day before. This caused an overestimation of turbulence and precluded the formation of a shallow inversion layer during night-time. In short the good simulation of a LLJ by MAR or not in December 2011 was mainly the result of the good behavior of turbulence or not in the model, which itself results mainly from a good behavior or not of the simulated cloud cover. LLJs are more sensitive to turbulence than the winds simulated near the surface. Consequently the evaluation of their behavior may help us in evaluating vertical mixing of chemical species. Of course a longer time serie must be analysed in order to confirm this result. Note that statistics of observed LLJs at Dome C are already given in Barral et al. (2014).

Hereafter we focus on a well marked case study which is accurately simulated, in order to infer in a deeper way how to evaluate the simulation of a LLJ by a 3D model.

3.2 The case study

We consider the same experiment as in Gallée et al. (2014, this issue) and the observations which have been performed on a 45 m tower with 6 levels of measurement (Genthon et al., 2010, 2013). The situation of 16–17 December 2011 has been chosen because the model simulates a low level jet at a height where it has been observed. An other case study occurring on 26 December 2011 evening is presented in Gallée et al. (2014, this issue). In that case the model overestimates significantly the height at which the LLJ is observed, mainly because it fails in simulating the surface energy balance during day-time, in conjunction with an underestimation of the cloud cover by the model. In contrast the simulated surface energy balance is much better simulated by MAR on 16 December, when the downward longwave radiation flux (DLW) is only slightly underestimated.

MAR simulation for 16–17 December 2011 is compared with observation on Fig. 2. The low level jet is simulated at 01:00 LT on 17 December at 14 m a.g.l. This height is comparable to that found in the observations (18 ± 4 m) as we have observations at 10.8, 18.2 and 25.6 m a.g.l. Both simulation and observation show a strong wind shear beneath the jet and almost no wind shear above. The temperature profiles are similar, with the same evolution of the intensity and depth of the inversion, although the depth is slightly underestimated.

Vertical profiles of simulated temperatures, wind speeds and wind directions are compared on Fig. 3 to the observations made at the tower for 16 h LT and 24 h LT. Temperatures are overestimated during day-time and overestimated above the LLJ during night-time. The overestimation above the LLJ during night-time may be due to an underestimation of turbulence by the E – e model. Similarly momentum mixing seems to be well simulated during day-time but the wind speed is underestimated at midnight above the LLJ, as the temperature. Possibly this is linked to the representation of large scale winds in the model (see Fig. 5). Wind direction seems to be well simulated.

The behaviour of MAR turbulent scheme is also discussed in Gallée et al. (2014, this issue) with the conclusion that the underestimation of turbulence may be partly due to the

underestimation of DLW, which is responsible for an overestimation of the vertical stability near the surface during night-time.

We now have a look at the general conditions prevailing during this LLJ.

The synoptic scale situation prevailing on 16–17 December in the vicinity of Dome C and illustrated by the 500 hPa geopotential map consists in a low pressure center situated on the Ross ice Shelf, with a secondary minimum on Adélie Land (see Fig. 4 for the situation at 12:00 UT on 16 December). Intensity of both diminishes with time while they remain stationary. Consequently the synoptic scale pressure gradient force is directed from the southwest to the northeast at Dome C while synoptic scale (geostrophic) winds blow from the Antarctic plateau towards Dome C during this period.

It appears that the model captures reasonably well the wind vector above the tower, as it can be seen from a comparison with the forcing (ERA-Interim) at 100 and 300 m a.g.l. The error in the wind speed and direction may amount respectively to 1.5 m/sec and 30^o (see Fig. 5). Note that universal time is used in the figure and that the crude time discretisation of ERA forcing (data provided each 6 hours only) influences strongly the time evolution of the simulated wind speed and direction. Indeed MAR data are provided with a time resolution of 10 min but exhibit significant changes only each 6 hours.

Lets now look at the simulation along the slope (x axis) and consider the pressure gradient force (PGF). Rather than representing the norm of the PGF horizontal vector ($\mathrm{PGF}_u, \mathrm{PGF}_v$) we represent the contribution of the PGF to the wind speed intensity (V). This allows us to get more insight into the role of the different forces in accelerating the wind speed at the end of day-time. This contribution may be obtained by multiplying the equations for u and v by u and v respectively and summing them in order to obtain an equation for the local variation of the kinetic energy with time.

We get (see appendix for more details):

$$\frac{\partial V}{\partial t} = \underbrace{\frac{u}{V}\mathrm{ADV}_u + \frac{v}{V}\mathrm{ADV}_v}_{\text{Advection Contribution}} + \underbrace{\frac{u}{V}\mathrm{PGF}_u + \frac{v}{V}\mathrm{PGF}_v}_{\text{PGF Contribution}} + \underbrace{\frac{u}{V}F_u + \frac{v}{V}F_v}_{\text{Turbulence Contribution}} \quad (1)$$

where ADV_u and ADV_v are the contributions from advection to u and v respectively. Similarly F_u and F_v are the contributions from turbulence. Of course the contribution of the Coriolis force to the kinetic energy is zero and so it is the same for the wind speed. Note also that a zero PGF contribution to the wind speed evolution should be related to the fact that the PGF vector is orthogonal to the wind vector.

Vertical profiles of advection, PGF, the contribution of turbulence and horizontal diffusion, and their sum at 16 h LT and 24 h LT are shown in Fig. 6. The last is interpreted as the tendency of the wind speed. These profiles are roughly homogeneous along the vertical during day-time (16 h LT), with PGF counterbalancing roughly the turbulent contribution. A similar equilibrium between PGF and turbulent contribution exists at midnight below the LLJ but their absolute values are reinforced. The contribution of turbulence is zero at the level of the LLJ and just above, where turbulence production by the wind shear is almost zero. Horizontal diffusion contributes negatively (positively) below (above) the height of the jet core. The negative contribution in the bulk of the boundary layer could be related to the weakening of the wind speed on the slope directed towards negative x values during night-time. The maximum in the wind speed tendency results from the dominant contribution of the PGF just above the boundary layer, i.e., where the contribution of turbulence cancels.

The wind speed V, the wind direction, the contribution of the pressure gradient force (PGF) to the wind speed and the direction of the PGF vector ($\mathrm{PGF}_u, \mathrm{PGF}_v$) simulated by the model are shown on Fig. 7a (day-time) and b (night-time). The (PGF contribution to the) wind speed and the direction of the wind speed (direction of the PGF vector) are shown respectively by contour lines and by colours.

A positive PGF contribution to the wind speed, as defined in Eq. (1), means that the PGF is responsible for an acceleration of the wind speed. The wind is roughly from the south-south-east during day-time (Fig. 7a, 16:00 LT). It comes from a slightly more southerly direction only above the jet level (14 m a.g.l.) during night-time (Fig. 7b, 24:00 LT) and blows from the south-west below. The changes in the wind direction between 16:00 and 24:00 LT result from a change in the direction of the synoptic scale PGF vector ($\mathrm{PGF}_{u,\mathrm{syn}}, \mathrm{PGF}_{v,\mathrm{syn}}$) from south-westerly to westerly. The wind direction well above the jet level 14 m a.g.l. was influ-

enced by turbulence at 16:00 LT, with a direction between the direction of the geostrophic wind (south-easterly) and that of the PGF vector (south-westerly). At 24:00 LT, it is no more influenced above the jet level by turbulence and comes in the geostrophic wind direction (southerly at that time), while below the jet level it is still influenced by turbulence and comes between the geostrophic wind direction and the PGF vector direction (westerly).

The reason why the PGF contributes to an acceleration of the wind speed up to 14 m a.g.l. at Dome C (isocontours of Fig. 7b, lower panel, at 24:00 LT and $x = 0$ km) comes from the fact that the wind direction is not geostrophic, because it is influenced by turbulence generated by surface friction up to this height. In fact turbulence deflects the wind vector, forcing it to blow from a direction in which it may be accelerated by the PGF. The acceleration occurs when turbulence shuts down at the end of the day. Then the increasing wind speed is responsible for an increase of the Coriolis force and the wind starts to turn to the left (anti-clockwise rotation). This is not the case above 14 m, where the wind direction is close to be geostrophic, i.e., the wind vector is roughly perpendicular to the PGF vector.

Note on Fig. 7b the weakening of the wind speed below the jet level (14 m a.g.l.) from day to night, which is due to a strong weakening of turbulence led by a strong increase of the vertical stability of the atmosphere. In contrast the onset of a low level jet is responsible for an increase of the vertical wind shear between the ground and 14 m a.g.l., so that the weakening of turbulence from day to night may be slightly limited. In fact a possible contribution of the low level jet to turbulence in our case seems not significant. Rather turbulence during night-time on 16–17 December 2014 is essentially generated by the surface friction. Also the strong stabillity of the atmosphere at Dome C during night-time explains why the LLJ is situated very close to the surface and may be observed over a relatively short tower.

Note also the occurrence of the wind speed maxima with downslope wind direction just above 14 m a.g.l. at 24:00 LT (see e.g., Fig. 7b, top panel, $x = -200$ km and $x = 130$ km). These maxima may correspond to an acceleration of the wind when turbulence in the boundary layer weakens, so that the downslope flow behaves like an advective-gravity flow (see Mahrt, 1982).

The component of the PGF along the x axis (PGF_u) on 16 December at 24:00 LT is compared to the temperature on Fig. 8a. It is found that PGF_u intensifies below 14 m a.g.l. except between -150 and 0 km, where the local slope is in the opposite direction of its general direction. The variations of PGF_u along the x axis below 14 m a.g.l. occur in conjunction with a strong inversion, suggesting that they are associated with a downslope pressure gradient force. The variations of PGF_u also influence the variations of the contribution of the PGF to the wind speed (Fig. 7b, bottom). Nevertheless neither the wind speed nor the wind direction are strongly affected by these variations (Fig. 7b, top). Inversion winds are generated by the downslope pressure gradient force. The thickness of the layer over which such a circulation occurs is generally no larger than a few tens of meters. Here the pressure gradient force is homogeneous along the vertical up to 2500 m a.g.l., suggesting that the synoptic scale pressure gradient force is responsible for the general direction and intensity of the wind during that time. In other words the inversion winds are not responsible for the wind field at Dome C during the LLJ case of 16–17 December 2014.

Note that the height of the strong inversion layer is the smallest and the inversion the strongest over the Dome (Fig. 8), probably because of a progressive weakening of the flow which is counteracted upstream by the downlope contribution of the PGF along the x axis, leading to a minimum in the wind speed and subsequently in the turbulent kinetic energy there. Probably the mass divergence caused by inversion winds all around Dome C during night-time also played a role.

The contribution of the PGF to the wind speed is also compared with the air temperature on Fig. 8b. From the discussion above it appears that the change of sign of this contribution at Dome C (i.e., a change in the PGF contribution from an acceleration of the wind speed below 14 m a.g.l. to a slight deceleration above – pay attention to the colour scale) is not fortuitous. The 14 m a.g.l. level at Dome C is situated just below the sign reversal, i.e., where PGF still contributes to an acceleration of the wind speed. As the turbulence has already shut down there (see Fig. 6), we get good conditions for the formation of a low level jet.

In fact the coincidence between the height of the change of sign of PGF contribution to the wind speed and the top of the inversion layer during night-time may be due to a wind

vector no longer orthogonal to the PGF in the inversion layer, but partly directed in the same direction as the wind vector. This is because turbulence there is generated by surface friction (Ekman Wind) at that time. As a remnant of the wind direction change due to turbulence still exists in the upper part of the inversion layer, while turbulence contribution has already shut down, the PGF is in position to accelerate the wind speed there.

Figure 9 illustrates the sudden shut-down of turbulence 14 m a.g.l. at Dome C after 19:00 LT, while the PGF is sustained. Such a situation has already been described by Blackadar (1957) as a source of an inertial oscillation. Indeed it is found that the wind vector at 14 m a.g.l. initiates a counter clock-wise rotation typical of an inertial oscillation until midnight-time (Fig. 10). This inertial oscillation is initiated by the sudden acceleration of the wind speed arising in conjunction with the sudden shut-down of turbulence. Contrary to the observations the inertial oscillation vanishes around 01:30 LT in the model. A possible cause is that turbulence is again active at that time (Fig. 9). Another possible explanation is that the horizontal diffusion of the model damps the inertial oscillation as it does above 14 m a.g.l.

Advection weakens between 18 h LT and 21 h LT and recovers after that time. The weakening of advection occurs mainly below 20 m a.g.l. and decreases progressively upwards. It is found that turbulence is larger to the South of (upstream) Dome C than at Dome C at 14 m a.g.l. (height of the jet core) and at 19 h LT, while this is not the case at 22 h LT. Also at 19 h LT the wind speed is larger upstream Dome C than at Dome C. But at 17 h LT the contribution of turbulence is smaller everywhere at 14 m a.g.l. while the wind speed is already larger upstream Dome C. A possible mechanism upstream Dome C could be a slight reinforcement of the wind speed during day-time by an upslope PGF, leading to a larger wind shear and turbulence there at the end of the day. While the inertial oscillation starts at Dome C due to the shutdown of turbulence, this is not yet the case upstream. Turbulence shuts down there only a few hours later. Consequently the advection of momentum at Dome C could be weaker during a few hours at the end at the day. In short if surface temperature is overestimated by the model the reinforcement of the wind speed and turbulence upstream Dome C during day-time could be overestimated by the model, and could lead to

an overestimation of turbulence during a few hours at the end of day-time, a subsequent underestimation of advection at Dome C at the height of the LLJ and an underestimation of its strength.

4 Conclusions

MAR simulates a low level jet at Dome C on 16–17 December 2011, as in the observations. It is the first time that a 3-D simulation of such a low level jet (LLJ) over an ice sheet is performed. The good behaviour of the model allows us to perform an analysis of the dynamical contributions (PGF, turbulence, advection) to the simulated wind speed.

It appears that the low level jet (LLJ) is generated when turbulence shuts down at the end of day-time, just above the turbulent layer, where the flow is still deflected from the geostrophic wind direction, blowing from higher to lower pressures. The low level jet seems not to be due to inversion winds over Dome C, but a reinforced low level jet is simulated by the model over the slopes near Dome C, where and when the downslope PGF reinforces the synoptic scale PGF. In contrast the model is not able to simulate the inertial oscillation after 01:30 LT. The cause is not yet firmly identified and this would be the subject of future work.

Finally the height of the LLJ at Dome C is strongly dependant on the height of the turbulent layer and thus its simulation is an indicator of the success or not of a model in simulating the intensity of turbulence under stable conditions. Cuxart et al. (2006) and Barral et al. (2014) show that a model overestimating turbulence overestimates the height of the wind speed maximum. Here a slight underestimation of turbulence by MAR possibly due to a slight underestimation of the downward long-wave radiation flux during night-time is responsible for a possible slight underestimation of the LLJ height. Vertical stratification of the atmosphere is strongly stable at Dome C during night-time, even in summer. During day-time the sensible heat fluxes are much larger than the latent heat fluxes, because of the low temperature and the subsequent very low capacity of the atmosphere to contain water (see e.g., King et al., 2006). Consequently the conditions for developing a well mixed

layer during day-time are optimal. This means that the simulation of summer case studies at Dome C could help a lot in validating the turbulence scheme of an atmospheric model. Due to its particular location and available set of observations, Dome C was recently selected as the test site for the next Gewex Atmospheric Boundary Layer Studies (GABLS4) model intercomparison (see http://www.cnrm.meteo.fr/aladin/meshtml/GABLS4/GABLS4.html).

Appendix A: Contributions to the wind speed

Equations of horizontal motion in MAR read (Gallée and Schayes, 1994):

$$\frac{\partial u}{\partial t} = -u\frac{\partial u}{\partial x} - v\frac{\partial u}{\partial y} - \dot{\sigma}\frac{\partial u}{\partial \sigma} + fv - \left.\frac{\partial \phi}{\partial x}\right|_p + F_u \tag{A1}$$

$$\frac{\partial v}{\partial t} = -u\frac{\partial v}{\partial x} - v\frac{\partial v}{\partial y} - \dot{\sigma}\frac{\partial v}{\partial \sigma} - fu - \left.\frac{\partial \phi}{\partial y}\right|_p + F_v \tag{A2}$$

where f is the Coriolis parameter, $\phi = gz$ is the geopotential, and F_u and F_v are the contributions of turbulence to the wind components u and v respectively. Writing

$$\mathrm{ADV}_u = -u\frac{\partial u}{\partial x} - v\frac{\partial u}{\partial y} - \dot{\sigma}\frac{\partial u}{\partial \sigma}$$

$$\mathrm{ADV}_v = -u\frac{\partial v}{\partial x} - v\frac{\partial v}{\partial y} - \dot{\sigma}\frac{\partial v}{\partial \sigma}$$

$$\mathrm{PGF}_u = -\left.\frac{\partial \phi}{\partial x}\right|_p$$

$$\mathrm{PGF}_v = -\left.\frac{\partial \phi}{\partial y}\right|_p$$

and multiplying the first equation by u and the second by v one gets the equation for the horizontal kinetic energy

$$u\frac{\partial u}{\partial t} + v\frac{\partial v}{\partial t} = u\mathsf{ADV}_u + v\mathsf{ADV}_v + u\mathsf{PGF}_u + v\mathsf{PGF}_v + uF_u + vF_v \tag{A3}$$

where

$$u\frac{\partial u}{\partial t} + v\frac{\partial v}{\partial t} = V\frac{\partial V}{\partial t}$$

dividing both members of the equation for the horizontal kinetic energy by V one gets

$$\frac{\partial V}{\partial t} = \underbrace{\frac{u}{V}\mathsf{ADV}_u + \frac{v}{V}\mathsf{ADV}_v}_{\text{Advection Contribution}} + \underbrace{\frac{u}{V}\mathsf{PGF}_u + \frac{v}{V}\mathsf{PGF}_v}_{\text{PGF Contribution}} + \underbrace{\frac{u}{V}F_u + \frac{v}{V}F_v}_{\text{Turbulence Contribution}} \tag{A4}$$

Appendix: Acknowlegments

The OPALE project was funded by the ANR (Agence National de Recherche) contract ANR-09-BLAN-0226.

Most of the computations presented in this paper were performed using the Froggy platform of the CIMENT infrastructure (https://ciment.ujf-grenoble.fr), which is supported by the Rhône-Alpes region (GRANT CPER07_13 CIRA), the OSUG@2020 labex (reference ANR10 LABX56) and the Equip@Meso project (reference ANR-10-EQPX-29-01) of the programme Investissements d'Avenir supervised by the Agence Nationale pour la Recherche.

This work was also granted access to the HPC resources of IDRIS under the allocation 2014–1523 made by GENCI.

IPEV-CALVA, INSU-LEFE-CLAPA and OSUG GLACIOCLIM-CENACLAM projects are acknowledged for their support.

References

Andreas, E. L., Claffey, K. J. and Makshtas, A. P.: Low-level atmospheric jets and inversions over the western Weddell sea, Bound.-Lay. Meteorol., 97, 459–486, 2000.

Banta, R. M., Pichugina, Y. L., and Newsom, R. K.: Relationship between low-level jet properties and turbulence kinetic energy in the nocturnal stable boundary layer, J. Atmos. Sci., 60, 2549–2555, 2003.

Barral, H., Vignon, E., Genthon, C., Bazile, E., Traullé, O., Gallée, H., Brun, C., Couvreux, F., and Le Moigne., P.: Summer diurnal cycle at Dome C on the Antarctic plateau, in: Proceeding of the AMS 21st Symposium on Boundary Layers and Turbulence, 9–13 June 2014, Leeds, UK, poster session 1, paper 14, 2014.

Bintanja, R.: Snowdrift suspension and atmospheric turbulence. Part I: Theoretical background and model description, Bound.-Lay. Meteorol., 95, 343–368, 2000.

Blackadar, A. K.: Boundary layer wind maxima and their significance for the growth of nocturnal inversions, B. Am. Meteorol. Soc., 38, 283–290, 1957.

Cuxart, J., Holtslag, A.A.M., Beare, R.J., Bazile, E., Beljaars, A., Cheng, A., Conangla, L., Ek, M., Freedman, F., Hamdi, R., Kerstein, A., Kitagawa, H., Lenderink, G., Lewellen, D., Mailhot, J., Mauritsen, T., Perov, V., Schayes, G., Steeneveld, G-J., Svensson, G., 2006.Taylor, P., Weng, W., Wunsch, S. and Xu, K-M.: Single-Column Model Intercomparison for a Stably Stratified Atmospheric Boundary Layer, Bound.-Lay. Meteorol., 118(2), 273-303,

Cuxart, J. and Jimenez, M. A.: Mixing processes in a nocturnal low-level jet: an LES study, J. Atmos. Sci., 64, 1666–1679, 2007.

Davies, P A.: Development and mechanisms of the nocturnal jet, Meteorol. Appl., 7, 239–246, 2000.

Duynkerke, P. G. and Driedonks, A. G. M.: A model for the turbulent structure of the stratocumulus-topped atmospheric boundary layer, J. Atmos. Sci., 44, 43–64, 1987.

Gallée, H.: Simulation of the mesocyclonic activity in the Ross Sea, Antarctica, Mon. Weather Rev., 123, 2051–2069, 1995.

Gallée, H. and Schayes, G.: Development of a three-dimensional meso-gamma primitive equations model, katabatic winds simulation in the area of Terra Nova Bay, Antarctica, Mon. Weather Rev., 122, 671–685, 1994.

Gallée, H., Preunkert, S., Argentini, S., Frey, M. M., Genthon, C., Jourdain, B., Pietroni, I., Casasanta, G., Barral, H., Vignon, E., and Legrand, M.: Characterization of the boundary layer at Dome C during OPALE, Atmos. Chem. Phys. Discuss., submitted, 2014.

Genthon, C., Town, M. S., Six, D., Favier, V., Argentini, S., and Pellegrini, A.: Meteorological atmospheric boundary layer measurements and ECMWF analyses during summer at Dome C, Antarctica, J. Geophys. Res.-Atmos., 115, D05104, doi:10.1029/2009JD012741, 2010.

Genthon, C., Six, D., Gallée, H., Grigioni, P., and Pellegrini, A.: Two years of atmospheric boundary layer observations on a 45 m tower at Dome C on the Antarctic plateau, J. Geophys. Res.-Atmos., 118, 3218–3232, doi:10.1002/jgrd.50128, 2013.

King, J. C., Argentini, S., and Anderson, P. S.: Contrasts between the summertime surface energy balance and boundary layer structure at Dome C and Halley stations, Antarctica, J. Geophys. Res.-Atmos., 111, D02105, doi:10.1029/2005JD006130, 2006.

Mahrt, L.: Momentum balance of gravity flows, J. Atmos. Sci., 39, 2701–2711, 1982.

Neff, W., Helmig, D., Grachev, A., and Davis, D.: A study of boundary layer behavior associated with high NO concentrations at the South Pole using a minisodar, tethered balloon, and sonic anemometer, Atmos. Environm., 42, 2762-2779.

Sukoriansky, S., Galperin, P., and Veniamin, P.: Application of a new spectral theory on stably stratified turbulence to the atmospheric boundary layer over sea ice, Bound.-Lay. Meteorol., 117, 231–257, 2005.

Van de Wiel, B. J. H., Moene, A. F., Steeneveld, G. J., Baas, P., Bosveld, F. C., and Holtslag, A. A. M.: A Conceptual View on Inertial Oscillations and Nocturnal Low-Level Jets, J. Atmos. Sci., 67, 2679–2689, doi:10.1175/2010JAS3289.1, 2010.

Observation				Simulation			
Date		h (m)	LLJ (m/s)	Date		h (m)	LLJ (m/s)
12 Dec	21h00	18.2	4.33	13 Dec	00h00	08.0	4.34
14 Dec	03h30	18.2	3.26	14 Dec	04h30	10.0	3.80
15 Dec	00h00	25.6	5.40	15 Dec	01h00	10.0	5.44
16 Dec	01h00	18.2	5.59	16 Dec	01h00	08.0	4.83
17 Dec	01h00	18.2	7.56	17 Dec	02h00	14.0	6.52
17 Dec	23 h 30	32.9	8.53	18 Dec	00h30	22.0	8.26
22 Dec	05h30	25.6	6.40	22 Dec	05h30	14.0	4.22
22 Dec	00h30	18.2	1.02	22 Dec	23h30	10.0	3.68
25 Dec	00h00	18.2	6.47	25 Dec	00h00	16.0	6.85
26 Dec	04h30	25.6	7.70	26 Dec	04h30	16.0	5.72
26 Dec	06h00	25.6	6.14				
27 Dec	00h30	18.2	6.59				
28 Dec	02h30	32.9	7.12				
28 Dec	04h00	18.2	6.72				
29 Dec	04h30	25.6	10.6				

Table 1. Observed and simulated LLJs at Dome C during OPALE. h is the height of the LLJ.

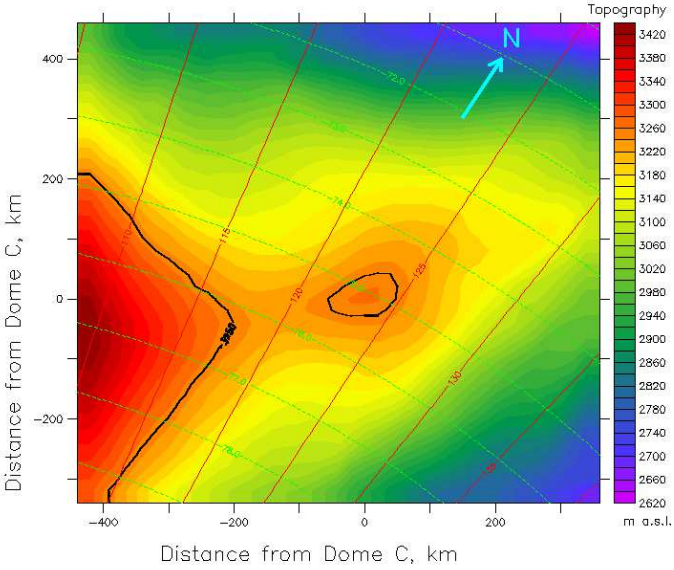

Figure 1. MAR integration domain and topography (color). Solid line represents the 3250 m isocontour.

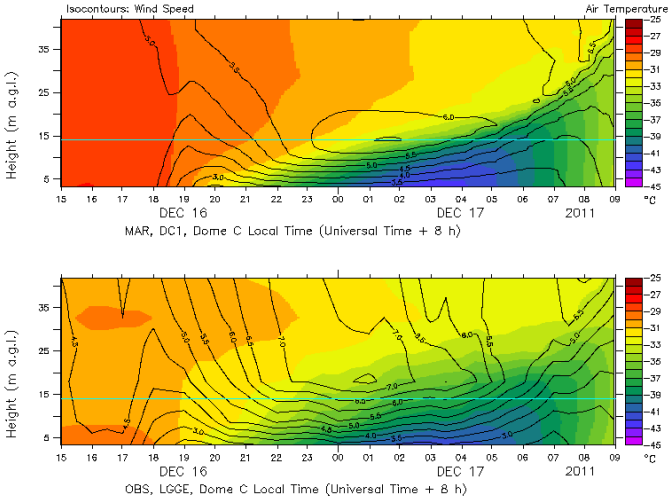

Figure 2. Temperature (color) and wind speed (isocontours) at Dome C tower, simulated by MAR on 16–17 December 2011 (upper panel) and observed (lower panel). Local Time LT (Universal Time UT $+ 8$ h) is used. The simulated jet level is at $z = 14$ m a.g.l. (shown by a cyan line in both panels).

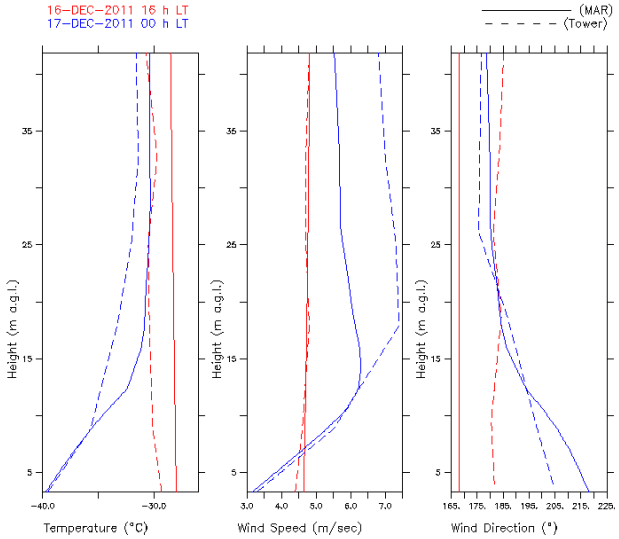

Figure 3. Vertical profiles of simulated temperatures, wind speeds and wind directions on 16 December 2011 at 16 h LT and midnight.

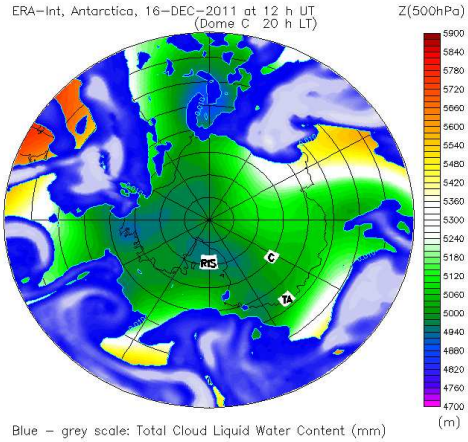

Figure 4. 500 hPa geopotential (m) over Antarctica on 16 December 2011 at 12:00 UT (color key to the right). Total cloud liquid water content (TCLW), from 0.01 (dark blue) to 1.2 mm (grey) is also shown. TCLW 0.01 mm isocontour is also represented by cyan line. Dome C is indicated by letter C. Terre Adélie and the Ross Ice Shelf are indicated respectively by "TA" and "RIS".

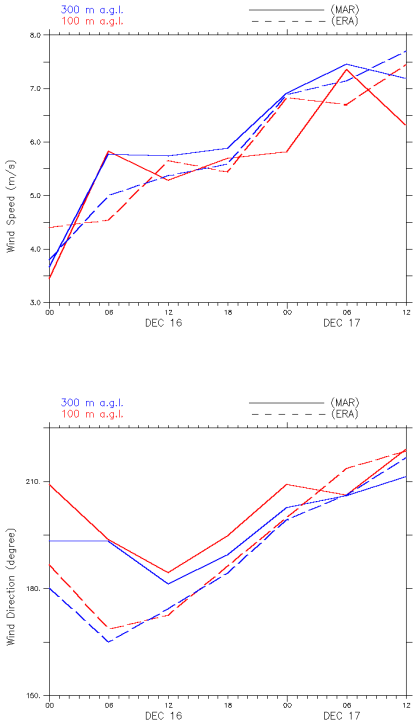

Figure 5. Comparaison beween the analysed wind speed (top) and direction (bottom) and the simulation, at 100 m a.g.l. and 300 m a.g.l. Note that universal time is used.

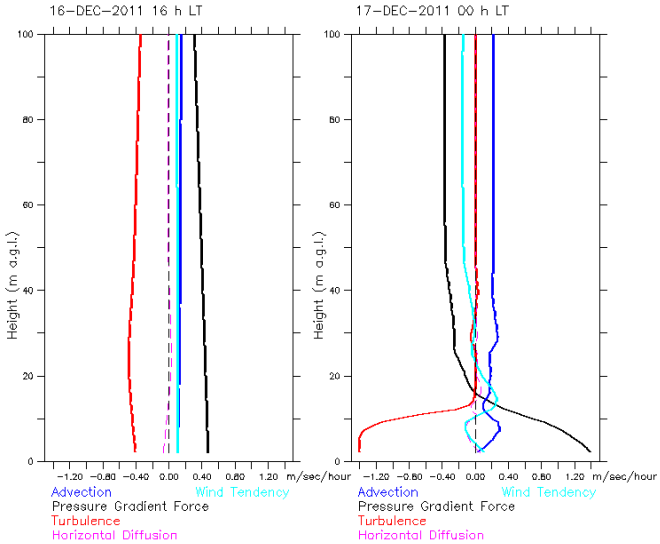

Figure 6. Vertical profiles of the contributions to the wind speed of PGF, advection, turbulence and horizontal diffusion.

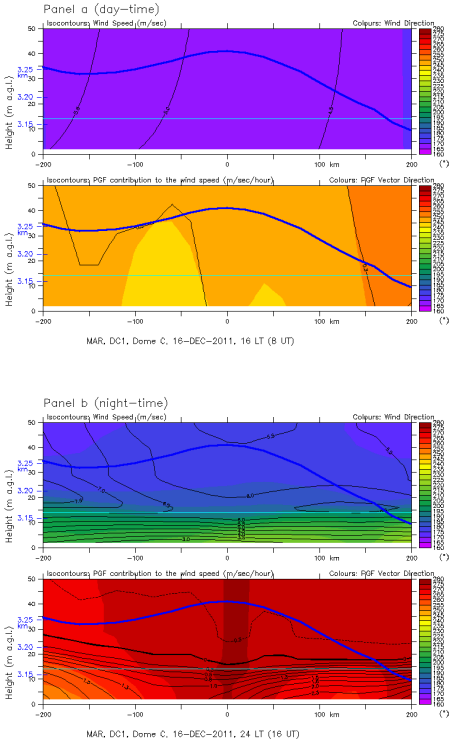

Figure 7. (a) Wind (top) and PGF(bottom) at the end of day-time (16:00 LT), along the x axis. The PGF contribution to the wind speed is defined in Eq. (1). PGF Vector refers to (PGF_u, PGF_v). Domain topography is shown by the thick blue line. Distance from Dome C is in km. The simulated jet level is at $z = 14$ m a.g.l. (cyan line). **(b)** same as in **(a)**, but at midnight.

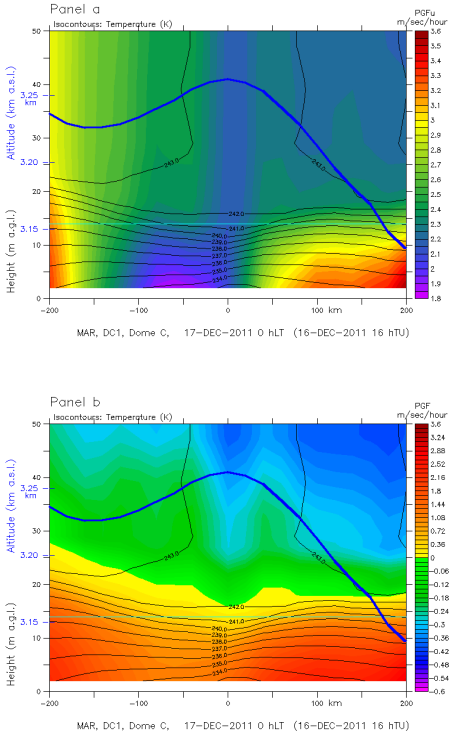

Figure 8. (a) Temperature and PGF_u at midnight, along the x axis. Distance is from Dome C. **(b)** Temperature and PGF, at midnight, along the x axis. Distance is from Dome C.

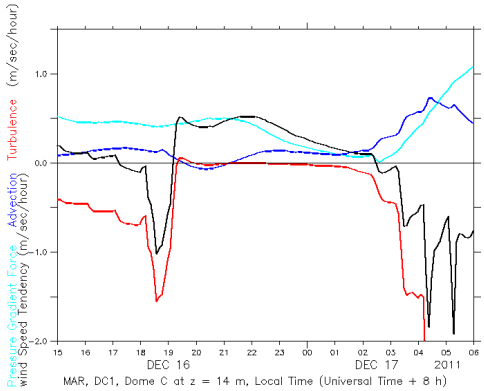

Figure 9. Simulated contribution of the forces to the wind speed, 14 m a.g.l. at Dome C on 16–17 December 2011. Local Time LT (Universal Time UT + 8 h) is used. The shutdown of turbulence occurs at 19:00 LT.

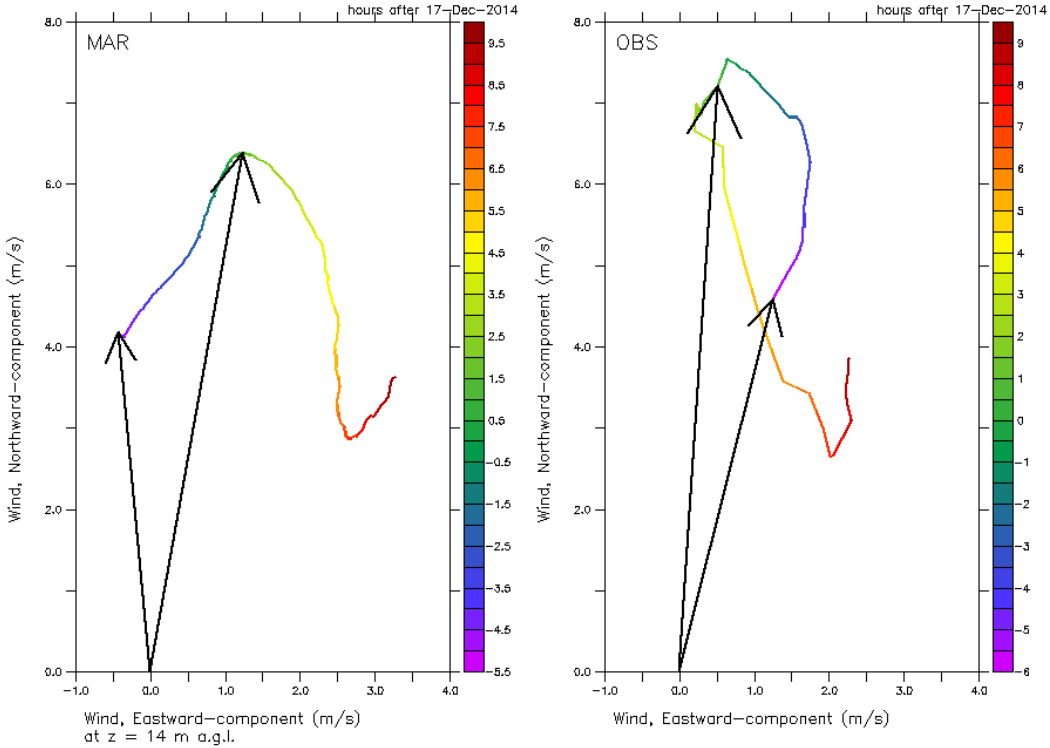

Figure 10. Wind hodograph at Dome C between 16 December 2011 19:00 LT and 17 December 2011 10:00 LT. Colours represent time in hours before/after 17 December midnight (negative/positive values). Arrows are plotted for 16 December 2011 19:00 LT and 17 December 2011 01:30 LT. Panel labeled "MAR": simulation at $z = 14$ m a.g.l. Panel labeled "OBS": observations at level 3 of the tower ($z = 17.9$ m a.g.l.).